NJC

Accepted Manuscript

This article can be cited before page numbers have been issued, to do this please use: M. B. Morelli, C. Amantini, G. Santoni, M. Pellei, C. Santini, C. Cimarelli, E. Marcantoni, M. Petrini, F. Del Bello, G. Giorgioni, A. Piergentili and W. Quaglia, *New J. Chem.*, 2018, DOI: 10.1039/C8NJ01763H.

This is an Accepted Manuscript, which has been through the Royal Society of Chemistry peer review process and has been accepted for publication.

Accepted Manuscripts are published online shortly after acceptance, before technical editing, formatting and proof reading. Using this free service, authors can make their results available to the community, in citable form, before we publish the edited article. We will replace this Accepted Manuscript with the edited and formatted Advance Article as soon as it is available.

You can find more information about Accepted Manuscripts in the author guidelines.

Please note that technical editing may introduce minor changes to the text and/or graphics, which may alter content. The journal's standard Terms & Conditions and the ethical guidelines, outlined in our author and reviewer resource centre, still apply. In no event shall the Royal Society of Chemistry be held responsible for any errors or omissions in this Accepted Manuscript or any consequences arising from the use of any information it contains.

ROYAL SOCIETY OF CHEMISTRY

rsc.li/njc

View Article Online
DOI: 10.1039/C8NJ01763H

Novel antitumor copper(II) complexes rationally designed to act through synergistic mechanisms of action, due to the presence of an NMDA receptor ligand and copper in the same chemical entity

Maria Beatrice Morelli,[†,a] Consuelo Amantini,[†,b] Giorgio Santoni,[a] Maura Pellei,[*,c] Carlo Santini,[c] Cristina Cimarelli,[c] Enrico Marcantoni,[c] Marino Petrini,[c] Fabio Del Bello,[*,d] Gianfabio Giorgioni[d] Alessandro Piergentili,[d] and Wilma Quaglia[d]

[a]*School of Pharmacy, ImmunoPathology and Molecular Medicine Unit, University of Camerino, via Madonna delle Carceri 9, 62032 Camerino, Italy*

[b]*School of Biosciences and Veterinary Medicine, University of Camerino, via Madonna delle Carceri 9, 62032 Camerino, Italy*

[c]*School of Science and Technology, Chemistry Division, University of Camerino, via S. Agostino 1, 62032 Camerino, Italy*

[d]*School of Pharmacy, Medicinal Chemistry Unit, University of Camerino, via S. Agostino 1, 62032 Camerino, Italy*

[†]These authors contributed equally to this work.

*Corresponding authors: E-mail addresses: fabio.delbello@unicam.it (F. Del Bello), maura.pellei@unicam.it (M. Pellei)

View Article Online
DOI: 10.1039/C8NJ01763H

Abstract

In the present article the 1,4-dioxane derivative **1**, a potent noncompetitive NMDA receptor antagonist, showed cytotoxic activity in MCF7 breast cancer cell line significantly higher than those of the functionally related compounds (*S*)-(+)-ketamine and MK-801. Encouraged by this result and considering that copper complexes have been highlighted to be promising anticancer agents, the NMDA receptor ligand **1** was linked to the bifunctionalizable species **2** and **3**, affording the conjugated derivatives **4** and **5** that were used for the preparation of the stable Cu(II) complexes **6** and **7**. All the compounds were evaluated against a panel of human cancer cell lines derived from solid tumors. Complex **7** showed the best antitumor activity in all the studied cell lines. This result suggests that **7** might act through synergistic mechanisms of action due to the presence of the NMDA ligand **1** and copper(II) in the same chemical entity. Furthermore, the cellular mechanisms affected by complex **7** were assessed through cytofluorimetric and western blot analyses. Data suggested the induction of cell death through paraptosis mediated by the endoplasmatic reticulum (ER) stress.

Abbreviations: CNS, central nervous system; mGluRs, metabotropic glutamate receptors; iGluRs, ionotropic glutamate receptors; NMDA, N-methyl-D-aspartate; AMPA, α-amino-3-hydroxy-5-methyl-4-isoxazolepropionic acid; KA, 2-carboxy-3-carboxymethyl-4-isopropenylpyrrolidine; PCP, phencyclidine; PI, propidium iodide; DCFDA, dichlorodihydrofluorescein diacetate; JC-1, 5,5',6,6'-tetrachloro-1,1',3,3'-tetraethyl-imidacarbocyanine iodide; CDI, carbonyldiimidazole; MTT, 3-(4,5-dimethylthiazol-2-yl)-2,5-diphenyl tetrazolium bromide; SRB, Sulforhodamine B; S.E., standard error.

View Article Online
DOI: 10.1039/C8NJ01763H

Introduction

Glutamate is a nonessential amino acid anion which behaves as the main excitatory neurotransmitter in the central nervous system (CNS), where it is involved in several physiological events.[1] The functions of glutamate are mediated by two classes of receptors, namely metabotropic glutamate receptors (mGluRs), which belong to the superfamily of G-protein coupled receptors and ionotropic glutamate receptors (iGluRs), which are ion channels.[2] Based on agonists selectively activating iGluRs, these receptors are further classified into N-methyl-D-aspartate (NMDA), α-amino-3-hydroxy-5-methyl-4-isoxazolepropionic acid (AMPA), and 2-carboxy-3-carboxymethyl-4-isopropenylpyrrolidine (kainate, KA) receptors.[3, 4] Among iGluRs, only NMDA receptors require binding of two co-agonists (glutamate and glycine) for their activation.[5, 6] They are cation channels with high calcium permeability, which are assembled by tetrameric combination of seven subunits, namely GluN1, GluN2A-D, GluN3A-B, encoded by separate genes.[7] The opening of the NMDA receptor-associated ion channel is controlled by various ligands interacting with different binding sites at the receptor, including binding site for glutamate, glycine, polyamines, Zn^{2+}, Mg^{2+}, H^{+}, as well as phencyclidine (PCP). This last binding site is located within the cation channel and compounds interacting with the PCP site behave as noncompetitive NMDA receptor antagonists.[8]

NMDA receptors are mainly present in neurons and play an important role in the development of CNS for the generation of rhythms for breathing and locomotion, and for the regulation of processes underlying learning, memory, and neuron maturation.[9, 10] Consequently, altered NMDA receptor expression and/or function are implicated in several neurological diseases. NMDA receptors have also been characterized for their surface expression and role in different types of cancer models.[11] In particular, GluN1 subunit is highly expressed in small-cell lung, as well as in cancerous colon or prostate cancer cell lines, while its expression is very low or absent in normal prostate tissue and benign prostate hyperplasia. Different combinations or single subunits of NMDA receptors have been observed in colon, oral, lung, prostate, and thyroid

cancer cell lines, as well as in laryngeal, gastric, esophageal, and hepatocellular carcinomas.[11, 12] Moreover, it has been demonstrated that breast cancer cells MCF7 and SKBR3 express NMDA GluN1 and GluN2B subunit mRNA and the noncompetitive NMDA receptor antagonist MK-801 reduced cell viability on both cell lines. MK-801 also inhibited tumor growth of MCF7 tumor xenografts in nu/nu mice, suggesting the active role played by NMDA receptor in breast cancer survival and growth.[13] We have recently reported that the 1,4-dioxane nucleus, which has already proved to be a suitable scaffold for building ligands selectively targeting different receptor systems,[14-21] is also compatible with ligands able to interact with NMDA receptor.[22] In particular, derivative **1** (Fig. 1) proved to be a potent noncompetitive NMDA receptor antagonist, showing K_i and IC_{50} values (712 nM and 24.2 nM, respectively) similar to those of the dissociative anaesthetic (*S*)-(+)-ketamine (K_i = 419 nM and IC_{50} = 11.4 nM).[22]

Based on these observations, to get more information about the role of NMDA receptor in breast cancer, in the present study we preliminarily evaluated the cytotoxic effect of **1** on MCF7 breast cancer cell line in comparison to those of the functionally related compounds (*S*)-(+)-ketamine and MK-801, by using the MTT assay. Interestingly, the 1,4-dioxane derivative **1** showed significant decrease in MCF7 cell viability with IC_{50} value of 70 μM, remarkably lower than those of MK-801 (IC_{50} = 328 μM) and (*S*)-(+)-ketamine (IC_{50} = 715 μM). Encouraged by this result, to further improve the antitumor activity of **1**, in the present study we designed to functionalize it with metal coordinating ligands, in order to form stable copper(II) complexes. Indeed, copper complexes have been highlighted to be promising anticancer agents, due to the elevated need for copper by cancer tissues and the established role of copper as a limiting factor for multiple aspects of tumor progression, including growth, angiogenesis and metastasis.[23-27] For this reason, they might represent efficacious alternatives to platinum-based drugs.[28-32] Recent anticancer screening of copper(I/II) complexes showed promising *in vitro* and *in vivo* results.[26, 33-41] Moreover, there is increasing evidence that the mechanism of action of copper complexes is distinctly different from cisplatin.[42] Copper complexes show broader spectra of activities and

View Article Online
DOI: 10.1039/C8NJ01763H

lower toxicity, thereby providing the possibility of circumventing the problems encountered by platinum drugs.[43, 44]

To obtain the novel metal complexes, compound **1** was first conjugated to the bifunctionalizable species **2** and **3**, affording derivatives **4** and **5** (Fig. 1). Compounds **2** and **3** were selected as coordinating agents based on the observation that bis(azol-1-yl)carboxylic acids are convenient starting materials for the synthesis of conjugated heteroscorpionate systems,[45-47] due to the k^3-NNO coordination behavior[48] of bis(azol-1-yl)methanes[49] and to the presence of a carboxylic function suitable for the coupling with the primary amine group of **1**. We have recently reported that heteroscorpionate ligands, obtained by conjugating **3** with nitroimidazole and glucosamine, and their related copper(II) complexes showed cytotoxic activity towards a panel of several human tumor cell lines.[50, 51]

The derivatives **4** and **5** were used for the preparation of the copper(II) complexes **6** and **7**, respectively (Fig. 1), which based on our hypothesis should act through synergistic mechanisms of action, due to the presence of the NMDA ligand **1** and copper(II) in the same chemical entity, with a desirable improvement of the cytotoxic activity.

The cytotoxicity profiles of both the copper(II) complexes **6** and **7**, as well as the corresponding uncoordinated ligands **1**-**5**, were evaluated *in vitro* on a panel of human tumor cell lines derived from different solid tumors. Moreover, the antitumor profile of complex **7** was deepened to investigate the type of cell death in MCF7 cell line, highly expressing NMDA receptor.

View Article Online
DOI: 10.1039/C8NJ01763H

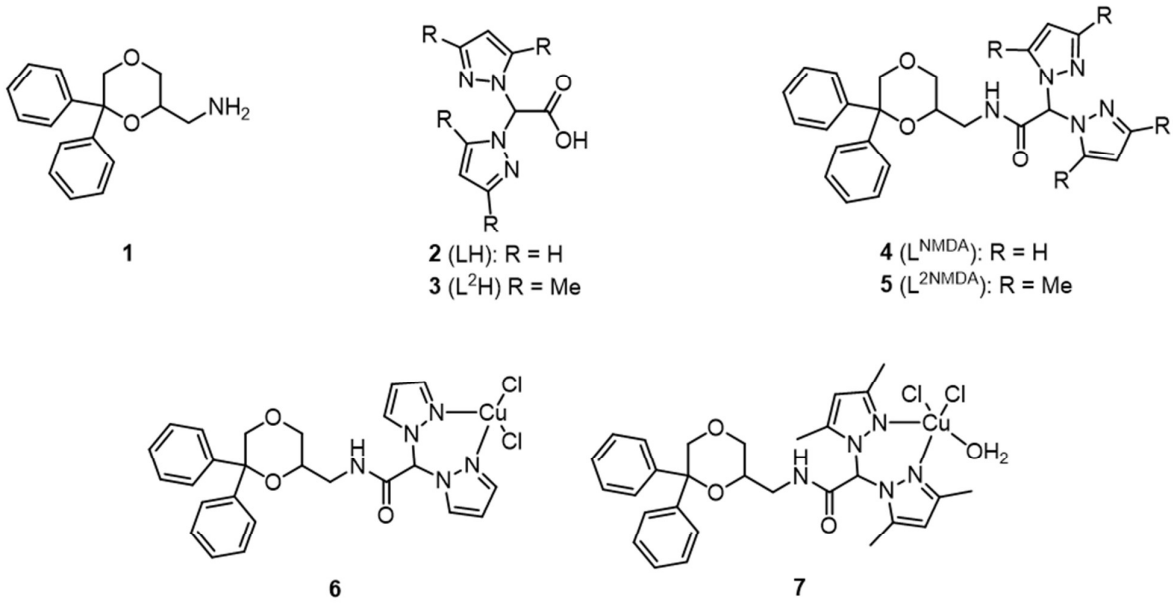

Fig. 1. Chemical structures of compounds **1**-**7**.

Experimental section

Chemistry

Materials and general methods

All solvents were dried, degassed and distilled prior to use. Elemental analyses (C,H,N,S) were performed in-house with a Fisons Instruments 1108 CHNS-O Elemental Analyser. Melting points were taken on an SMP3 Stuart Scientific Instrument. IR spectra were recorded from 4000 to 100 cm^{-1} with a Perkin-Elmer SPECTRUM ONE System FT-IR instrument. IR annotations used: br = broad, m = medium, s = strong, w = weak. ^1H NMR spectra were recorded on an Oxford-400 Varian spectrometer (400.4 MHz). Chemical shifts, in ppm, for ^1H NMR spectra are related to internal Me_4Si standard. NMR annotations used: d = doublet, m = multiplet, s = singlet, s br = broad singlet. Electrospray ionization mass spectra (ESI-MS) were obtained in positive- (ESI(+)MS) or negative-ion (ESI(-)MS) mode on a Series 1100 MSD detector HP spectrometer, using a methanol or acetonitrile mobile phase. The compounds were added to

reagent grade methanol to give solutions of approximate 0.1 mM concentration. These solutions were injected (1 μL) into the spectrometer via a HPLC HP 1090 Series II fitted with an autosampler. The pump delivered the solutions to the mass spectrometer source at a flow rate of 300 μL min^{-1}, and nitrogen was employed both as a drying and nebulising gas. Capillary voltages were typically 4000 V and 3500 V for the positive- and negative-ion mode, respectively. Confirmation of all major species in this ESI-MS study was aided by comparison of the observed and predicted isotope distribution patterns, the latter calculated using the IsoPro 3.0 computer program.

Synthesis

All reagents were purchased from Aldrich and used without further purification. The ligands **1**,[22] **2** (LH, $[HC(CO_2H)(pz)_2]$)[52] and **3** (L^2H, $[HC(CO_2H)(pz^{Me2})_2]$)[53] were prepared according to literature method.

*Synthesis of **4** (L^{NMDA})*

Carbonyldiimidazole (CDI, 0.302 g, 1.860 mmol) was added to a solution of **2** (LH) (0.357 g, 1.860 mmol) in THF. The reaction mixture was stirred at reflux for 2 h, then it was cooled to 0°C. After **1** was added (0.501 g, 1.860 mmol), the solution was stirred at room temperature for 3 h. After evaporation of the solvent, the oil formed was dissolved in $CHCl_3$ and washed with $NaHCO_3$ saturated solution and 2N HCl. The $CHCl_3$ phase was dried over Na_2SO_4. The evaporation of the solvent under reduced pressure gave a solid, which was purified by column chromatography, eluting with cyclohexane/ethyl acetate (5:5). Yield: 47%. Mp. 172-173°C. ^1H NMR ($CDCl_3$, 293K): δ 3.37-3.76 (m, 6H, dioxan and CH_2N), 4.58 (d, 1H, dioxan), 6.35 (m, 2H, 4-C*H*), 7.10 (s, 1H, C*H*), 7.18-7.39 (m, 14H, Ar*H*, 3-C*H* and 5-C*H*), 7.83 (s br, 1H, N*H*). IR (cm^{-1}): 3287br (NH); 3121w, 3103w, 3052w, 3026w, 2978w, 2935w, 2915w, 2860w (CH); 1682s (C=O); 1560m (C=N); 1516w, 1495m, 1451m, 1432m, 1388m, 1350w, 1312m, 1293m, 1271m, 1244m, 1211w, 1188w, 1163w, 1122s, 1088s, 1065s, 1050s, 1026m, 1000m, 991s, 958m, 916s, 886w, 858m, 844m, 809s, 766s, 750s, 729s, 705s, 694s, 661m. ESI-MS (major positive-ions,

CH_3CN), *m/z* (%): 444 (100) $[L^{NMDA} + H]^+$. ESI-MS (major negative-ions, CH_3CN), *m/z* (%): 442 (100) $[L^{NMDA} - H]^-$. Calcd. for $C_{25}H_{25}N_5O_3$: C, 67.70; H, 5.68; N, 15.79%. Found: C, 67.38; H, 5.75; N, 15.50%.

Synthesis of ***5*** *(L^{2NMDA})*

This compound was prepared starting from **3** (L^2H) following the procedure described for **2**. The residue was purified by column chromatography, eluting with cyclohexane/ethyl acetate (7:3), to give a white solid. Y Yield: 54%. Mp. 171-172°C. ^{1}H NMR ($CDCl_3$, 293K): δ 2.10 (s, 3H, C*H*$_3$), 2.13 (s, 3H, C*H*$_3$), 2.38 (s, 3H, C*H*$_3$), 2.39 (s, 3H, C*H*$_3$), 3.30-3.79 (m, 6H, dioxan and C*H*$_2$N), 4.61 (d, 1H, dioxan), 5.84 (s, 1H, 4-C*H*), 5.85 (s, 1H, 4-C*H*), 6.77 (s, 1H, C*H*), 7.18-7.39 (m, 10H, Ar*H*), 8.10 (s br, 1H, N*H*). IR (cm^{-1}): 3423w (NH); 3090w, 3062w, 2985w, 2961w, 2926w, 2907w, 2869w (CH); 1702s (C=O); 1568m (C=N); 1520s, 1465m, 1446s, 1415m, 1372m, 1364m, 1335w, 1316m, 1295m, 1260m, 1240m, 1221w, 1128m, 1102s, 1064s, 1028m, 998m, 985m, 940m, 919m, 874m, 835m, 814m, 799m, 773s, 757s, 739s, 722m, 707s, 698s, 663m. ESI-MS (major positive-ions, CH_3OH), *m/z* (%): 1022 (100) $[2L^{2NMDA} + Na]^+$; 522 (20) $[L^{2NMDA} + Na]^+$. ESI-MS (major negative-ions, CH_3OH), *m/z* (%): 498 (100) $[L^{2NMDA} - H]$. Calcd. for $C_{29}H_{33}N_5O_3$: C, 69.72; H, 6.66; N, 14.02%. Found: C, 69.93; H, 6.85; N, 13.81%.

Synthesis of ***6*** *[(L^{NMDA})$CuCl_2$]*

$CuCl_2{\cdot}2H_2O$ (0.006 g, 0.338 mmol) was added to a methanol suspension (25 mL) of **4** (L^{NMDA}, 0.015 g, 0.338 mmol). The reaction mixture was stirred at room temperature for 12 h to obtain a light blue precipitate, which was filtered, washed with acetonitrile and dried under vacuum to give the cyan complex **6** ([(L^{NMDA})$CuCl_2$]) in 61% yield. Mp. 232-235°C. IR (cm^{-1}): 3274w (NH); 3112w, 3053w, 2979w, 2957w, 2916w, 2859w (CH); 1678s (C=O); 1567m (C=N); 1509w, 1492w, 1452m, 1427w, 1401m, 1366w, 1325w, 1307w, 1283m, 1239m, 1202w, 1127m, 1093m, 1065s, 1051m, 1026w, 1001w, 985m, 936m, 915w, 899w, 889w, 865w, 845m, 830m, 747s, 726m, 706s, 694m, 662m. ESI-MS (major positive-ions, CH_3OH/DMSO (10:1)), *m/z* (%): 984 (50) $[(L^{NMDA})_2CuCl]^+$. ESI-MS (major negative-ions, CH_3OH), *m/z* (%): 170 (100) $[CuCl_3]^-$,

478 (70) [L^{NMDA} + Cl]$^-$. Calcd. for $C_{25}H_{25}Cl_2CuN_5O_3$: C, 51.95; H, 4.36; N, 12.12%. Found: C, 52.00; H, 4.40; N, 12.45%.

Synthesis of 7 [(L^{2NMDA})$CuCl_2$]·H_2O

This compound was prepared starting from **5** (L^{2NMDA}) following the procedure described for **6**. The obtained light blue solution was evaporated and the residue was washed with acetonitrile and dried under vacuum to give the brown complex **7** ([(L^{2NMDA})$CuCl_2$]·H_2O) in 65% yield. Mp. 194°C dec. IR (cm^{-1}): 3432br (OH); 3198br, 3058w, 3024w, 2968br, 2904br (CH); 1667s (C=O); 1562s (C=N); 1490w, 1460m, 1448m, 1418m, 1395m, 1351w, 1311m, 1247m, 1226m, 1126m, 1106m, 1062m, 1050m, 1026m, 989m, 935w, 900m, 874m, 859w, 796w, 767m, 753m, 729m, 700s, 665m. ESI-MS (major positive-ions, CH_3OH), *m/z* (%): 531 (100) [(L^{2NMDA})$_2$Cu]$^{++}$. ESI-MS (major negative-ions, CH_3OH), *m/z* (%): 170 (100) [$CuCl_3$]$^-$, 247 (25) [L^2]$^-$. Calcd. for $C_{29}H_{35}Cl_2CuN_5O_4$: C, 53.42; H, 5.41; N, 10.74%. Found: C, 52.72; H, 5.20; N, 10.77%.

Experiments with human cultured cells

Copper complexes and the corresponding uncoordinated ligands were dissolved in DMSO. Cisplatin was dissolved in 0.9% sodium chloride solution. 3-(4,5-dimethylthiazol-2-yl)-2,5-diphenyltetrazolium bromide (MTT), Sulforhodamine B (SRB) and cisplatin were obtained from Sigma Chemical Co, St. Louis, USA.

Cell Cultures

Human PC3 prostate cancer, MCF7 and SKBR3 breast cancer, H460 non small cell lung cancer and T24 bladder cancer cell lines were obtained from American Type Culture Collection (ATCC, Rockville, MD). Human Caki-2 renal cancer cell line was purchased from Cell bank Interlab Cell Line Collection (ICLC, Italy). Cell lines were maintained in the logarithmic phase at 37°C in a 5% carbon dioxide atmosphere using the following culture media containing 10% fetal calf serum (Euroclone, Milan, Italy), antibiotics (50 units/mL penicillin and 50 µg/mL

DOI: 10.1039/C8NJ01763H

streptomycin), and 2 mM L-glutamine: RPMI-1640 medium (Euroclone) for MCF7 and T24 cells; DMEM medium (Euroclone) for SKBR3, H460, PC3 cells; McCoy medium (Euroclone) for Caki-2 cells.

MTT Assay

The growth inhibitory effect toward cancer cell lines was evaluated by colorimetric MTT assay. Briefly, (3–8) × 10^3 cells/well, dependent upon the growth characteristics of the cell line, were seeded in 96-well microplates in growth medium (100 µL). After 24 h, the medium was removed and replaced with fresh media containing the compound to be studied at the appropriate concentration. Triplicate cultures were established for each treatment. After 72 h, 0.8 mg/mL of MTT (Sigma Aldrich) was added to the samples and incubated for 3 h. Then the supernatants were discarded and coloured formazan crystals, dissolved with 100 µL/well of DMSO, were read at 570 nm by the enzyme-linked immunosorbent assay reader (BioTek Instruments, Winooski, USA). Four replicates were used for each treatment. IC_{50} values, showed as mean ± standard error (S.E.), correspond to the drug concentration that induces 50% of cell growth inhibition compared to untreated control wells. IC_{50} values were calculated using Prism 5.0a (Graph Pad).

SRB Assay

The growth inhibitory effects of compounds **6** and **7** toward cancer cell lines were also evaluated by colorimetric SRB assay. Cisplatin was used as reference agent. Briefly, cells were seeded in 96-well microplates as above described. After 24 h, the medium was removed and replaced with fresh media containing the compound to be studied at the appropriate concentration. At the same time, a plate was tested to evaluate the cell population before the compound addition (Tz). Triplicate cultures were established for each treatment. After 72 h, cells were fixed with cold trichloroacetic acid (TCA) and stained using 0.4% SRB (Sigma Aldrich) dissolved in 1% acetic acid. Bound stains were subsequently solubilized with 10 mM Trizma, and the absorbance was read on the microplate reader at 520 nm. The percentage of growth inhibition was calculated as

[(Ti - Tz)/(C - Tz)] × 100 for concentrations for which Ti > Tz or [(Ti - Tz)/Tz] × 100 for those for which Ti < Tz, where Tz = absorbance time zero, C = absorbance in the presence of vehicle, and Ti = absorbance in the presence of drug at different concentrations. Then three dose response parameters were calculated according to the National Cancer Institute guideline: the growth inhibition of 50% (GI_{50}), the total growth inhibition (TGI), and the 50% lethal concentration (LC_{50}).

Propidium iodide (PI) staining

After treatment with vehicle (control) or 25 μM complex **7** for 48 h, MCF7 cells were incubated in a binding buffer containing 20 μg/mL PI for 10 min at room temperature. The cells were then analyzed by flow cytometry using CellQuest software.

Apoptosis assays

The exposure of phosphatidylserine on MCF7 cells was detected by Annexin V staining and cytofluorimetric analysis. MCF7 cells were plated at the density of 1.25 x 10^5 cells/mL and treated for 48 h with vehicle (control) or 25 μM complex **7**. After treatment, the cells were stained with 5 μL of Annexin V FITC (Life Technologies Italia) for 10 min at room temperature, washed once with binding buffer and analyzed on a FACScan flow cytometer using CellQuest software.

Western blot assay

MCF7 cells, treated for 48 h with vehicle (control) or with 25 μM complex **7**, were lysed in a lysis buffer (1 M Tris pH 7.4, 1 M NaCl, 10 mM EGTA, 100 mM NaF, 100 mM Na_3V0_4, 100 mM fluoridefenilmetansulfonile, 2% deoxycholate, 100 mM EDTA, 10% triton X-100, 10% glycerol, 10% SDS, 0.1 M $Na_4P_2O_7$) supplemented with a protease inhibitor cocktail (Sigma Aldrich). Proteins were separated on 7-12% SDS polyacrylamide gel in a Mini-PROTEAN Tetra Cell system (BioRad, Italy). Protein transfer from the gel to a nitrocellulose membrane was carried out using Mini Trans-Blot Turbo RTA system (BioRad). Non-specific binding sites were blocked with 5% low-fat dry milk, 1% bovine serum albumin (BSA) in PBS with 0.1% tween 20

View Article Online
DOI: 10.1039/C8NJ01763H

for 1 h at room temperature. Then membranes were incubated overnight at 4°C in primary Abs: anti-human caspase 3 (1:1000, Cell Signaling), anti-human BiP (1:1000, Cell Signaling), and anti-human β actin (1:1000, Cell Signaling), followed by the incubation (room temperature, 1 h) with HRP-conjugated anti-rabbit or anti-mouse secondary Abs (1:2000, Cell Signaling). Peroxidase activity was visualized with the LiteAblot ®PLUS and LiteAblot® TURBO (EuroClone, Italy) kits and densitometric analysis was carried out by a Chemidoc using the Quantity One software (BioRad).

ROS production

The fluorescent probe dichlorodihydrofluorescein diacetate (DCFDA) was used to assess oxidative stress levels. Briefly, MCF7 cells were plated at the density of 1.25 x 10^5 cells/mL and treated for 48 h with vehicle (control) or 25 μM complex **7**. At the end of treatments, cells were incubated with DCFDA (Sigma Aldrich, Italy) for 20 min prior to the harvest time point at 37°C, 5% CO_2, and analyzed by FACScan cytofluorimeter using the Cell Quest software.

Mitochondrial transmembrane potential (ΔΨm)

Mitochondrial transmembrane potential (*ΔΨm)* was evaluated by 5,5',6,6'-tetrachloro-1,1',3,3'-tetraethyl-imidacarbocyanine iodide (JC-1) staining. Briefly, MCF7 cells were plated at the density of 1.25 x 10^5 cells/mL and treated for 48 h with vehicle (control) or 25 μM complex **7**. At the end of the treatment, cells were incubated for 10 min at room temperature with 10 μg/mL of JC-1 (Life Technologies Italia, Italy). JC-1 was excited by an argon laser (488 nm), and green (530 nrn)/red (>570 nrn) emission fluorescence was collected simultaneously. Carbonyl cyanide chlorophenylhydrazone protonophore, a mitochondrial uncoupler, was used as a positive control (data not shown). Samples were analyzed by a FACScan cytofluorimeter using the CellQuest software.

Statistical analysis

The statistical significance was determined by Student's t-test.

View Article Online
DOI: 10.1039/C8NJ01763H

Results and discussion

Synthesis and characterization

Ligands **4** (L^{NMDA}) and **5** (L^{2NMDA}) were prepared according to the procedure reported in Scheme 1. The acids **2** (LH) and **3** (L^2H)[52, 53] were activated with CDI and then treated with amine **1**.[22] After separation and purification by column chromatography, **4** and **5** were obtained in a reasonable yield and purity. The ligand **4** is soluble in acetonitrile, chloroform and DMSO, while **5** is soluble in methanol, acetonitrile, chloroform and DMSO.

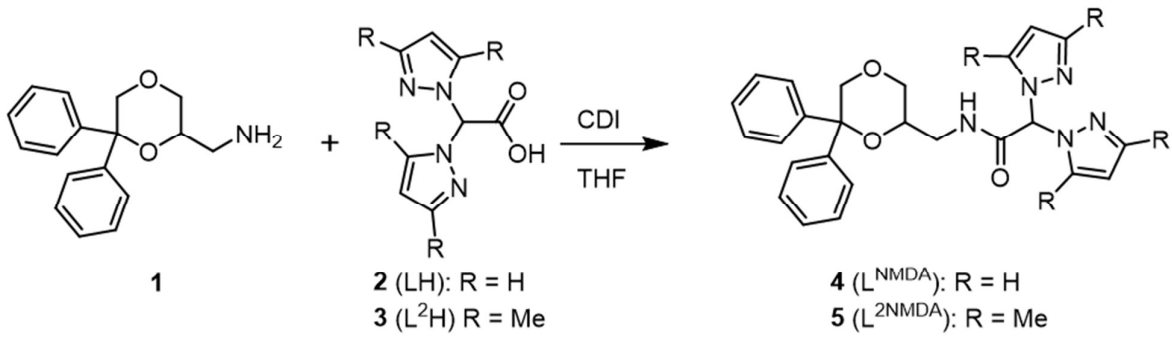

Scheme 1. Reaction scheme for the synthesis of ligands **4** and **5**.

The infrared spectra carried out on solid samples of **4** and **5** showed all the expected bands for the ligands: in particular, weak absorptions due to the CH stretching have been observed in the range 2860-3157 cm^{-1}, while peaks attributable to the amide stretching are present at 3287 cm^{-1} and 3423 cm^{-1}, respectively for L^{NMDA} and L^{2NMDA}. The asymmetric stretching of the C=O groups are detected as strong peaks at 1681 and 1702 cm^{-1}, respectively, in the typical range for the amide groups. The ^1H NMR spectra of **4** and **5**, recorded in $CDCl_3$ solution, showed all the expected signals for the bioconjugated ligands. Interestingly, a double set of resonances appears for the pyrazole rings, indicating that the pyrazoles are not equivalents. The ESI-MS study was

View Article Online
DOI: 10.1039/C8NJ01763H

conducted by dissolving the ligands **4** and **5** in acetonitrile and methanol, respectively, and recording the spectra in positive- and negative-ion mode. The molecular structures of **4** and **5** are confirmed by the presence of the molecular peak at *m/z* 442 and 498, attributable to the $[L^{NMDA} - H]^-$ and $[L^{2NMDA} - H]^-$ species, respectively, in the negative-ions spectra. The positive-ion spectrum of **4** also shows the molecular peak $[L^{NMDA} + H]^+$ at *m/z* 444, while in the spectrum of **5** the peaks at *m/z* 1022 and 522, relative to the species $[(L^{2NMDA})_2 + Na]^+$ and $[L^{2NMDA} + Na]^+$, respectively, are observed.

The copper complexes **6** $[(L^{NMDA})CuCl_2]$ and **7** $[(L^{2NMDA})CuCl_2{\cdot}H_2O]$ were prepared from the reaction of $CuCl_2{\cdot}2H_2O$ with **4** (L^{NMDA}) and **5** (L^{2NMDA}), respectively, in methanol suspension for **6** and in methanol solution for **7**, at room temperature (Scheme 2). Both compounds are soluble in DMSO, and **7** is also soluble in methanol, ethanol and chloroform.

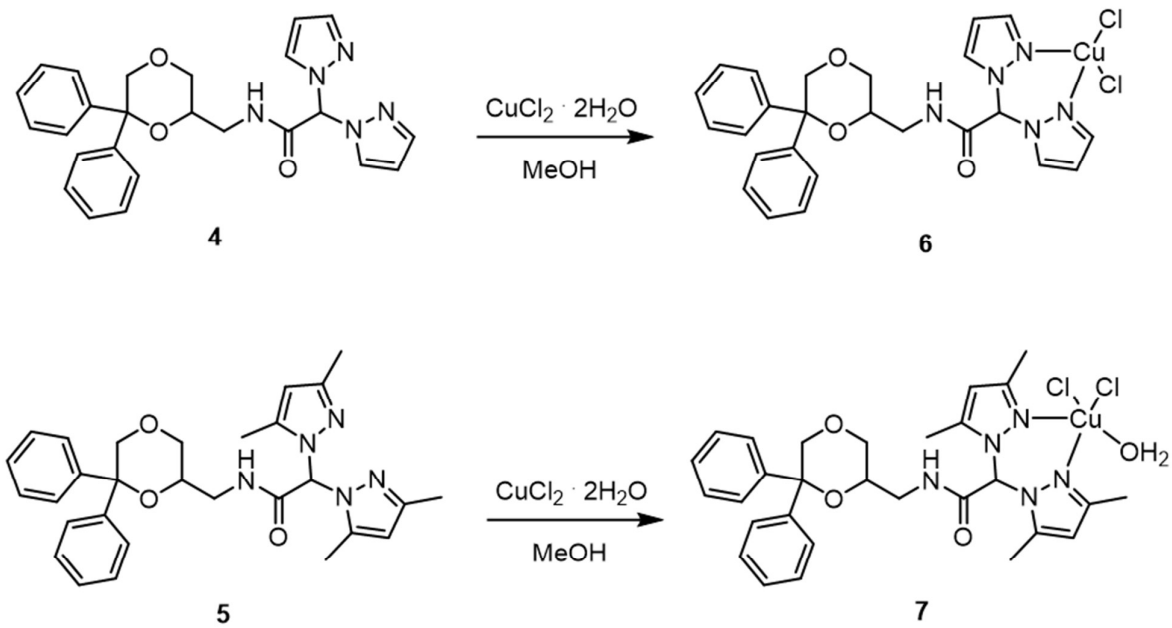

Scheme 2. Reaction scheme for the synthesis of complexes **6** and **7**.

The infrared spectra carried out on solid samples of **6** and **7** show all the expected bands for the complexes: the NH stretching is detected without a significant variation with a weak absorption

peak at 3274 cm^{-1} for **6** and a very broad absorption peak at 3432 cm^{-1} for **7**, indicating the presence of a molecule of water; weak absorptions are observed in the range 2859-3198 cm^{-1} due to the pyrazoles rings. The strong absorptions at 1678 and 1667 cm^{-1} for **6** and **7**, respectively, without a significant variation with respect to the absorptions detectable in the free ligands, indicate that the carbonyl groups are not involved in the coordination of the metal. The copper centre results in a tetracoordinated environment with the ligand chelating in a bidentate fashion and the other two positions occupied by the chlorides.

The ESI-MS study was conducted by dissolving compounds **6** and **7** in methanol/DMSO and methanol, respectively, and recording the spectra in positive- and negative-ion mode. In the positive ion spectrum of **6** it's possible to detect a major peak at *m/z* 984, attributable to the $[(L^{NMDA})_2CuCl]^+$ species, confirming the complex formation, while in the spectrum of **7** a peak at *m/z* 531 is attributable to the $[(L^{2NMDA})_2Cu]^{++}$ species. The negative-ion mode spectra of **6** and **7** show two peaks at *m/z* 478 and 247, attributable to the species $[L^{NMDA} + Cl]^-$ and $[L^2]^-$, respectively, confirming the presence of the ligands in the complexes.

Cell viability studies

The *in vitro* antitumor activity of the novel copper(II) complexes **6** and **7** and the uncoordinated ligands **1**-**5** was evaluated against a panel of human cancer cell lines derived from solid tumors. Cell growth was evaluated by means of the MTT test after 72 h exposure. The effects of the reference compound cisplatin, the most widely used anticancer metallodrug, were evaluated in the same experimental conditions. IC_{50} values, calculated from dose-response curves, are reported in Table 1.

Data analysis reveals that the NMDA receptor ligand **1** shows moderate antitumor effects not only on MCF7 breast cancer cell line (IC_{50} = 70 μM), but also on SKBR3, H460 and PC3 cell lines, with IC_{50} values ranging between 32 and 52 μM. Lower antitumor activity is observed in

View Article Online
DOI: 10.1039/C8NJ01763H

T24 and Caki-2 cells. On the contrary, bifunctionalizable coordinating compounds **2** and **3** proved to be unable to inhibit cell growth in all the studied tumor cell lines.

Table 1. *In vitro* antitumor activity of compounds **1-7** and cisplatin evaluated by MTT assay.

compound	IC_{50} (μM) ± S.E.					
	MCF7	SKBR3	H460	T24	PC3	Caki-2
1	70 ± 3.5	32 ± 1.8	34 ± 2.9	170 ± 5.3	52 ± 2.8	145 ± 5.8
2	ND	ND	ND	ND	ND	ND
3	ND	ND	ND	ND	ND	ND
4	148 ± 5.2	160 ± 4.3	144 ± 6.1	>300	>300	ND
5	49 ± 2.8	50 ± 2.1	31 ± 2.2	34 ± 2.1	53 ± 2.3	137 ± 4.9
6	107 ± 4.6	86 ± 3.7	60 ± 3.6	110 ± 4.5	85 ± 4.7	75 ± 3.4
7	25 ± 1.3	32 ± 1.9	15 ± 1.1	29 ± 2.0	21 ± 1.4	18 ± 1.7
cisplatin	8.3 ± 1.2	16 ± 1.5	1.6 ± 0.8	0.7 ± 0.1	10 ± 1.9	1.4 ± 0.7

S.E. = standard error. Cells were treated for 72 h with increasing concentrations of tested compounds. The statistical analysis of IC_{50} levels was performed using Prism 5.0a (Graph Pad). ND: not determinable.

The conjugation of **1** with **2** and **3**, affording **4** and **5**, respectively, produces different effects. Indeed, compared to **1**, the bis-pyrazolyl bioconjugated derivative **4** elicits a cell growth inhibitory activity significantly lower in all tumor cell lines, whereas the bis-3,5-dimethylpyrazolyl derivative **5** shows similar IC_{50} values in MCF7, SKBR3, H460, PC3 and Caki-2 cell lines, and even lower at T24 cells. Probably, the higher lipophilicity of **5**, due to the presence of methyl substituents on the pyrazolyl rings, might be responsible for the enhanced anticancer activity.

Interestingly, the final derivatives **6** and **7**, obtained by coordinating the conjugated derivatives **4** and **5** with copper(II), show IC_{50} values lower than those of the corresponding uncoordinated precursors in all the studied cell lines. Analogously to what observed for **4** and **5**, the bis-3,5-dimethylpyrazolyl derivative **7** proves to be more active than the corresponding unmethylated analog **6**, confirming the role played by the methyl groups on the antitumor activity of the compounds of the present article. Therefore, we can hypothesize that the physico-chemical

View Article Online
DOI: 10.1039/C8NJ01763H

properties of the bifunctionalizable species can also contribute to the inhibitory effect of the final complexes.

In all the studied cancer cell lines, except for SKBR3 cells, where the complex **7** and the NMDA receptor ligand **1** show similar cell growth inhibitory effects, **7** shows IC_{50} values lower than those of **1**. This result suggests that **7** might act through synergistic mechanisms of action due to the presence of the NMDA ligand **1** and copper(II) in the same chemical entity. The same interesting result was not obtained with complex **6**, probably because, as above discussed, the unmethylated bifunctionalizable species **2** negatively contributes to the antitumor activity.

The novel complexes **6** and **7**, along with cisplatin, were also evaluated by means of the SRB assay, to confirm the results obtained with MTT assay and get further information about the cytotoxic effect of these compounds. The antitumor activity was estimated by measurements of three parameters: GI_{50}, TGI and LC_{50} (Table 2).

Table 2. *In vitro* antitumor activity of compounds **6**, **7**, and cisplatin evaluated by SRB assay.

Cell line	(μM) ± S.E.	**6**	**7**	Cisplatin
MCF7	GI_{50}	46 ± 1.9	16 ± 1.9	5 ± 1.2
	TGI	140 ± 4.4	27 ± 3.2	21 ± 1.6
	LC_{50}	>300	48 ± 2.5	89 ± 3.7
SKBR3	GI_{50}	69 ± 4.8	15 ± 2.1	4.5 ± 0.7
	TGI	182 ± 6.9	27 ± 3.1	17 ± 2.4
	LC_{50}	>300	52 ± 3.6	63 ± 3.0
H460	GI_{50}	75 ± 5.2	27 ± 3.1	1.5 ± 0.3
	TGI	179 ± 8.1	47 ± 3.9	17 ± 2.8
	LC_{50}	>300	82 ± 4.2	198 ± 7.9
T24	GI_{50}	44 ± 4.2	17 ± 2.3	1.5 ± 0.5
	TGI	143 ± 5.4	31 ± 2.7	14 ± 2.1
	LC_{50}	>300	55 ± 4.2	143 ± 3.9
PC3	GI_{50}	52 ± 4.3	19 ± 2.4	4.7 ± 1.1
	TGI	127 ± 7.5	35 ± 3.6	17 ± 2.1
	LC_{50}	>300	67 ± 2.9	61 ± 4.3

View Article Online
DOI: 10.1039/C8NJ01763H

Caki-2	GI_{50}	101 ± 5.6	15 ± 2.7	3 ± 0.6
	TGI	176 ± 5.8	23 ± 3.4	8 ± 1.4
	LC_{50}	>300	35 ± 3.2	21 ± 1.3

S.E. = standard error. Growth Inhibition 50 (GI_{50}) represents the drug concentration (μM) required to inhibit 50% net of cell growth. Total Growth Inhibition (TGI) represents the drug concentration (μM) required to inhibit 100% of cell growth. Lethal Concentration 50 (LC_{50}) represents the drug concentration (μM) required to kill 50% of the initial cell number. Each quoted value represents the mean of quadruplicate determinations ± S.E. (n = 5).

The results reported in Table 2 show that the GI_{50} values of the tested compounds are not significantly different from the IC_{50} values obtained by means of the MTT assay, confirming that complex **7** is more active than **6** in all the studied cell lines. Moreover, compared to cisplatin, **7** shows higher GI_{50} value. Instead, considering LC_{50}, it is noteworthy that the cytotoxic effect of **7** is comparable to that of cisplatin on SKBR3, PC3 and Caki-2, and even higher on MCF7, H460 and T24 cells.

Complex **7**, showing the best activity profile on all the studied cell lines, was selected to better characterize its antitumor activity. To this aim, the type of cell death was investigated by treating MCF7 breast cancer cells, highly expressing NMDA receptors, for 48 h with 25 μM of **7** or vehicle (control). After treatment, cells were stained with PI or Annexin-V and then analyzed by cytofluorimetric analysis. As shown in Fig. 2A and B, compound **7** induced increase of PI fluorescence but not of Annexin V fluorescence compared with control cells suggesting that the type of cell death is not apoptosis.

To strengthen this data, we also performed western blot analysis to analyze cleavage of procaspase 3, an executioner caspase in apoptosis. Our results demonstrated that the treatment does not induce activation of caspase 3 as evidenced by the absence of caspase 3 cleaved fragments both in control and in complex **7**-treated MCF7 cells (Fig. 2C).

In addition, as it is well known that copper complexes stimulate cellular ROS formation,[54] MCF7 cells, treated as above described, were stained with DCFDA and analyzed by FACS. Our results

View Article Online
DOI: 10.1039/C8NJ01763H

showed that the treatment induces a marked increase in ROS production (MFI:16.49) with respect to control cells (MFI:6.85), indicating the induction of oxidative stress (Fig. 3A).

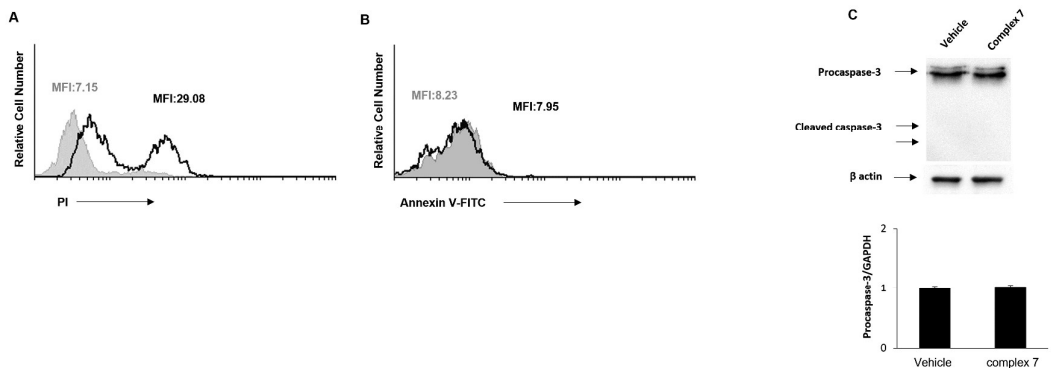

Fig. 2. Cytotoxic effects of complex **7** on MCF7 cells. A) Cell death was evaluated by PI staining and FACS analysis in MCF7 cells treated for 48 h with vehicle or with 25 μM complex **7**. Grey: Vehicle–treated cells; black: complex **7**-treated cells. MFI: Mean Fluorescence Intensity. Data are representative of at least three independent experiments. B) Annexin V-FITC staining was performed in MCF7 cells treated for 48 h with vehicle or with 25 μM complex **7** to evaluate apoptotic cell death by FACS analysis. Grey: Vehicle–treated cells; black: complex **7**-treated cells. MFI: Mean Fluorescence Intensity. Data are representative of at least three independent experiments. C) Representative immunoblot of procaspase-3 and activated caspase-3 expression in MCF7 cells treated with vehicle or with 25 μM complex **7** for 48 h. Densitometric values were normalized to β actin used as loading control. Data, shown as fold respect to vehicle-treated cells, represent the mean ± SD of three separates experiments.

Considering that ROS over-production is often associated with alterations of the mitochondrial transmembrane potential[55] and that mitochondria play a pivotal role in the cell death pathways, we decided to label control and treated MCF7 cells with JC-1, a cationic carbocyanine dye that accumulates in mitochondria. We found that treatment with complex **7** does not promote mitochondrial membrane depolarization (Fig. 3B) but, as demonstrated by the enhancement in the JC-1-aggregates, it induces mitochondrial hyperpolarization (Fig. 3C). Since ROS production is associated with Endoplasmatic Reticulum (ER) stress[56] and copper complexes can trigger protein misfolding,[40] we also assessed the expression of immunoglobulin heavy chain binding

View Article Online
DOI: 10.1039/C8NJ01763H

protein/glucose regulated protein 78 (BiP/Grp 78), one of the best characterized chaperones in the ER protein folding machinery. By western blot analysis we showed that the treatment with complex **7** markedly increased the expression of BiP with respect to control cells, indicating the induction of ER stress (Fig. 3D). Moreover, we analyzed vehicle and compound **7**-treated MCF7 cells for physical parameters by FACS. Side scattering and forward scattering showed an increase of cell complexity and size in treated cells as evidenced by the shift in the high complexity and size fraction of the cytogram (Fig. 3E).

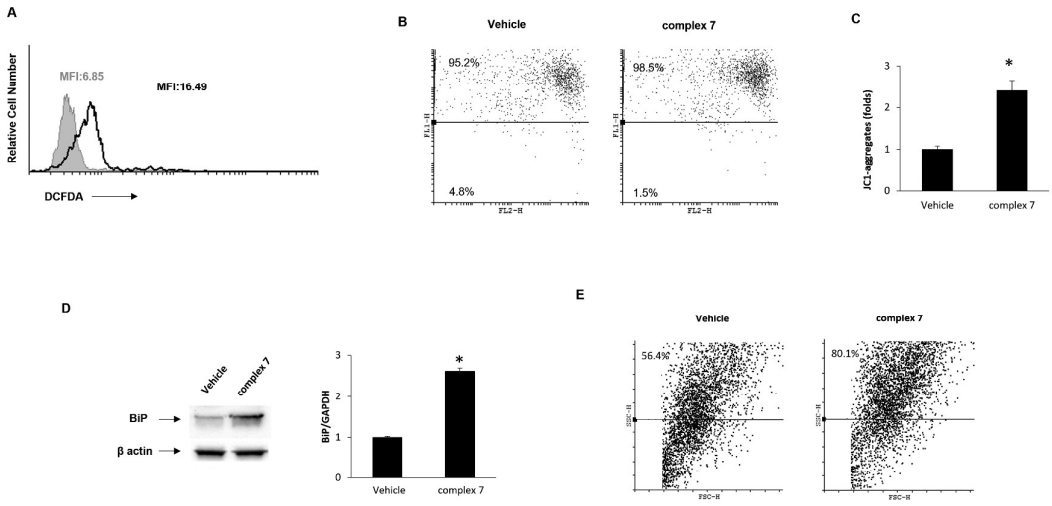

Fig. 3. Treatment with complex **7** induces ROS production, mitochondrial hyperpolarization and ER stress in MCF7 cells. A) ROS production was determined by cytofluorimetric analysis using DCFDA staining in MCF7 cells treated with vehicle or with 25 μM complex **7** for 48 h. Grey: Vehicle –treated cells; black: complex **7**-treated cells. MFI: Mean Fluorescence Intensity. Data are representative of at least three independent experiments. B) Changes in ΔΨm were evaluated by JC-1 staining and biparametric FL1(green)/FL2(red) flow cytometric analysis in MCF7 cells treated with vehicle or with 25 μM complex **7** for 48 h. Dot plots are representative of at least three independent experiments. Numbers indicate the percentage of cells in the upper and lower parts of the quadrants. C) JC-1 aggregates were measured by analyzing red fluorescence in MCF7 cells treated with vehicle or with 25 μM complex **7** for 48 h. Data, shown as fold respect to vehicle-treated cells, represent the mean ± SD of three separated experiments. *$p < 0.01$ vs vehicle-treated cells. D) Representative immunoblot of BiP expression in MCF7 cells treated with vehicle or with complex **7** for 48 h. Densitometric values were normalized to β actin used as loading control. Data, shown as fold respect to vehicle-treated cells, represent the mean ± SD of three separated experiments. *$p < 0.01$ vs vehicle-treated cells. E) Side scattering and forward scattering was evaluated by FACS analysis in MCF7 cells treated with vehicle or with 25 μM

DOI: 10.1039/C8NJ01763H

complex **7** for 48 h. Numbers indicate the percentage of cells in the upper part of the quadrant. Dot plots are representative of at least three independent experiments.

These morphological changes may occur during cytosolic vacuolization.[57] Overall, our data suggest that complex **7** exerts its cytotoxic activity by causing changes characteristic of paraptosis cell-death.

Conclusion

In summary, the noncompetitive NMDA receptor antagonist **1** shows antitumor activity at MCF7 breast cancer cell line significantly higher than those of the reference compounds (*S*)-(+)-ketamine and MK-801. Considering that copper complexes have also been demonstrated to be promising anticancer agents, ligand **1** was conjugated through an amide function with the bifunctionalizable species **2** and **3**, to form the conjugated derivatives **4** and **5** from which the novel copper(II) complexes **6** and **7** were obtained. Among the novel compounds, evaluated by MTT test against a panel of human tumor cell lines, the Cu(II) complex **7** shows the best antitumor activity in all the studied cells, suggesting that it might act through synergistic mechanisms of action due to the presence of the NMDA ligand **1** and Cu(II) in the same chemical entity. The results from SRB assay are comparable to those obtained with MTT test. Moreover, SRB assay allows to highlight that **7** shows LC_{50} values not significantly different from that of cisplatin on SKBR3, PC3 and Caki-2, and even higher on MCF7, H460 and T24 cells. Therefore, the working hypothesis was verified and **7** may represent a promising lead compound for the development of novel antitumor agents in which the cytotoxic effects of an NMDA receptor ligand and copper are combined. Finally, data obtained from the evaluation of mechanisms of the antitumor activity of **7** suggest that such a complex exerts its cytotoxic activity by causing changes characteristic of paraptosis cell-death, thus offering a new tool to overcome apoptosis resistance in breast cancer cells.

DOI: 10.1039/C8NJ01763H

Conflicts of interest

There are no conflicts to declare.

Acknowledgments

This work was supported by grants from the University of Camerino (Fondo di Ateneo per la Ricerca 2014-2015). We are grateful to CIRCMSB (Consorzio Interuniversitario di Ricerca in Chimica dei Metalli nei Sistemi Biologici).

References

1. B. S. Meldrum, *J. Nutr.*, 2000, **130**, 1007S-1015S.
2. A. Lau and M. Tymianski, *Pfluegers Arch.*, 2010, **460**, 525-542.
3. S. F. Traynelis, L. P. Wollmuth, C. J. McBain, F. S. Menniti, K. M. Vance, K. K. Ogden, K. B. Hansen, H. Yuan, S. J. Myers and R. Dingledine, *Pharmacol. Rev.*, 2010, **62**, 405-496.
4. D. Lodge, *Neuropharmacology*, 2009, **56**, 6-21.
5. R. Dingledine, N. W. Kleckner and C. J. McBain, in *Excitatory Amino Acids and Neuronal Plasticity*, ed. Y. Ben-Ari, Springer US, Boston, MA, 1990, DOI: 10.1007/978-1-4684-5769-8_3, pp. 17-26.
6. M. L. Blanke and A. M. J. Van Dongen, in *Biology of the NMDA Receptor*, ed. A. M. Van Dongen, CRC Press/Taylor & Francis, Boca Raton (FL), 2009, ch. 13, pp. 283-312.
7. A. Stepulak, R. Rola, K. Polberg and C. Ikonomidou, *J. Neural. Transm.*, 2014, **121**, 933-944.
8. S. E. Tomek, A. L. LaCrosse, N. E. Nemirovsky and M. Foster Olive, *Pharmaceuticals*, 2013, **6**, 251-268.

9. A. Sanz-Clemente, R. A. Nicoll and K. W. Roche, *Neuroscientist*, 2013, **19**, 62-75.

10. P. Paoletti, C. Bellone and Q. Zhou, *Nat. Rev. Neurosci.*, 2013, **14**, 383-400.

11. S. I. Deutsch, A. H. Tang, J. A. Burket and A. D. Benson, *Biomed. Pharmacother.*, 2014, **68**, 493-496.

12. A. Mehrotra and R. K. Koiri, *Int. J. Immunother. Cancer Res.*, 2015, **1**, 13-17.

13. W. G. North, G. Gao, V. A. Memoli, R. H. Pang and L. Lynch, *Breast Cancer Res. Treat.*, 2010, **122**, 307-314.

14. A. Piergentili, W. Quaglia, M. Giannella, F. Del Bello, B. Bruni, M. Buccioni, A. Carrieri and S. Ciattini, *Bioorg. Med. Chem.*, 2007, **15**, 886-896.

15. W. Quaglia, A. Piergentili, F. Del Bello, Y. Farande, M. Giannella, M. Pigini, G. Rafaiani, A. Carrieri, C. Amantini, R. Lucciarini, G. Santoni, E. Poggesi and A. Leonardi, *J. Med. Chem.*, 2008, **51**, 6359-6370.

16. F. Del Bello, E. Barocelli, S. Bertoni, A. Bonifazi, M. Camalli, G. Campi, M. Giannella, R. Matucci, M. Nesi, M. Pigini, W. Quaglia and A. Piergentili, *J. Med. Chem.*, 2012, **55**, 1783-1787.

17. V. Mammoli, A. Bonifazi, F. Del Bello, E. Diamanti, M. Giannella, A. L. Hudson, L. Mattioli, M. Perfumi, A. Piergentili, W. Quaglia, F. Titomanlio and M. Pigini, *Bioorg. Med. Chem.*, 2012, **20**, 2259-2265.

18. A. Bonifazi, A. Piergentili, F. Del Bello, Y. Farande, M. Giannella, M. Pigini, C. Amantini, M. Nabissi, V. Farfariello, G. Santoni, E. Poggesi, A. Leonardi, S. Menegon and W. Quaglia, *J. Med. Chem.*, 2013, **56**, 584-588.

19. F. Del Bello, A. Bonifazi, W. Quaglia, A. Mazzolari, E. Barocelli, S. Bertoni, R. Matucci, M. Nesi, A. Piergentili and G. Vistoli, *Bioorg. Med. Chem. Lett.*, 2014, **24**, 3255-3259.

20. F. Del Bello, A. Bonifazi, M. Giannella, G. Giorgioni, A. Piergentili, R. Petrelli, C. Cifani, M. V. Micioni Di Bonaventura, T. M. Keck, A. Mazzolari, G. Vistoli, A. Cilia, E. Poggesi, R. Matucci and W. Quaglia, *Eur. J. Med. Chem.*, 2017, **125**, 233-244.

21. F. Del Bello, A. Bonifazi, G. Giorgioni, R. Petrelli, W. Quaglia, A. Altomare, A. Falcicchio, R. Matucci, G. Vistoli and A. Piergentili, *Eur. J. Med. Chem.*, 2017, **137**, 327-337.

22. A. Bonifazi, F. Del Bello, V. Mammoli, A. Piergentili, R. Petrelli, C. Cimarelli, M. Pellei, D. Schepmann, B. Wünsch, E. Barocelli, S. Bertoni, L. Flammini, C. Amantini, M. Nabissi, G. Santoni, G. Vistoli and W. Quaglia, *J. Med. Chem.*, 2015, **58**, 8601-8615.

23. D. Denoyer, S. Masaldan, S. La Fontaine and M. A. Cater, *Metallomics*, 2015, **7**, 1459-1476.

24. V. Gandin, A. Trenti, M. Porchia, F. Tisato, M. Giorgetti, I. Zanusso, L. Trevisi and C. Marzano, *Metallomics*, 2015, **7**, 1497-1507.

25. C. Silva-Platas, C. E. Guerrero-Beltrán, M. Carrancá, E. C. Castillo, J. Bernal-Ramírez, Y. Oropeza-Almazán, L. N. González, R. Rojo, L. E. Martínez, J. Valiente-Banuet, L. Ruiz-Azuara, M. E. Bravo-Gómez, N. García, K. Carvajal and G. García-Rivas, *J. Bioenerg. Biomembr.*, 2016, **48**, 43-54.

26. V. Gandin, C. Ceresa, G. Esposito, S. Indraccolo, M. Porchia, F. Tisato, C. Santini, M. Pellei and C. Marzano, *Sci. Rep.*, 2017, **7**, 13936.

27. C. M. Weekley and C. He, *Curr. Opin. Chem. Biol.*, 2017, **37**, 26-32.

28. S. Medici, M. Peana, V. M. Nurchi, J. I. Lachowicz, G. Crisponi and M. A. Zoroddu, *Coord. Chem. Rev.*, 2015, **284**, 329-350.

29. C. Santini, M. Pellei, V. Gandin, M. Porchia, F. Tisato and C. Marzano, *Chem. Rev.*, 2014, **114**, 815-862.

30. F. Tisato, C. Marzano, M. Porchia, M. Pellei and C. Santini, *Med. Res. Rev.*, 2010, **30**, 708-749.

31. C. Marzano, M. Pellei, F. Tisato and C. Santini, *Anti-Cancer Agents Med. Chem.*, 2009, **9**, 185-211.

32. M. Wehbe, A. W. Y. Leung, M. J. Abrams, C. Orvig and M. B. Bally, *Dalton Transactions*, 2017, **46**, 10758-10773.

33. Q.-P. Qin, Y.-C. Liu, H.-L. Wang, J.-L. Qin, F.-J. Cheng, S.-F. Tang and H. Liang, *Metallomics*, 2015, **7**, 1124-1136.

34. N. Raman, R. Jeyamurugan, R. Senthilkumar, B. Rajkapoor and S. G. Franzblau, *Eur. J. Med. Chem.*, 2010, **45**, 5438-5451.

35. D. Palanimuthu, S. V. Shinde, K. Somasundaram and A. G. Samuelson, *J. Med. Chem.*, 2013, **56**, 722-734.

36. D. Montagner, B. Fresch, K. Browne, V. Gandin and A. Erxleben, *Chem. Commun.*, 2017, **53**, 134-137.

37. K. Laws, G. Bineva-Todd, A. Eskandari, C. Lu, N. O'Reilly and K. Suntharalingam, *Angew. Chem., Int. Ed.*, 2018, **57**, 287-291.

38. D. Mahendiran, R. S. Kumar, V. Viswanathan, D. Velmurugan and A. K. Rahiman, *JBIC, J. Biol. Inorg. Chem.*, 2017, **22**, 1109-1122.

39. L. Becco, J. C. García-Ramos, L. R. Azuara, D. Gambino and B. Garat, *Biol. Trace Elem. Res.*, 2014, **161**, 210-215.

40. V. Gandin, M. Pellei, F. Tisato, M. Porchia, C. Santini and C. Marzano, *J. Cell. Mol. Med.*, 2012, **16**, 142-151.

41. V. Gandin, F. Tisato, A. Dolmella, M. Pellei, C. Santini, M. Giorgetti, C. Marzano and M. Porchia, *J. Med. Chem.*, 2014, **57**, 4745-4760.

42. M. Zaki, F. Arjmand and S. Tabassum, *Inorg. Chim. Acta*, 2016, **444**, 1-22.

43. C. S. Allardyce and P. J. Dyson, *Dalton Trans.*, 2016, **45**, 3201-3209.

44. S. Spreckelmeyer, C. Orvig and A. Casini, *Molecules*, 2014, **19**, 15584-15610.

45. S. Trofimenko, *Scorpionates: The Coordination Chemistry of Poly(pyrazolyl)borate Ligands*, Imperial College Press, London, 1999.

46. C. Santini, M. Pellei, G. Gioia Lobbia and G. Papini, *Mini-Rev. Org. Chem.*, 2010, **7**, 84-124.

47. M. Pellei, G. Gioia Lobbia, G. Papini and C. Santini, *Mini-Rev. Org. Chem.*, 2010, **7**, 173-203.

48. A. Otero, J. Fernández-Baeza, A. Lara-Sánchez and L. F. Sánchez-Barba, *Coord. Chem. Rev.*, 2013, **257**, 1806-1868.

49. I. Alkorta, R. M. Claramunt, E. Díez-Barra, J. Elguero, A. de la Hoz and C. López, *Coord. Chem. Rev.*, 2017, **339**, 153-182.

50. M. Pellei, G. Papini, A. Trasatti, M. Giorgetti, D. Tonelli, M. Minicucci, C. Marzano, V. Gandin, G. Aquilanti, A. Dolmella and C. Santini, *Dalton Trans.*, 2011, **40**, 9877-9888.

51. M. Giorgetti, S. Tonelli, A. Zanelli, G. Aquilanti, M. Pellei and C. Santini, *Polyhedron*, 2012, **48**, 174-180.

52. N. Burzlaff, I. Hegelmann and B. Weibert, *J. Organomet. Chem.*, 2001, **626**, 16-23.

53. A. Beck, B. Weibert and N. Burzlaff, *Eur. J. Inorg. Chem.*, 2001, 521-527.

54. G. Filomeni, G. Cerchiaro, A. M. Da Costa Ferreira, A. De Martino, J. Z. Pedersen, G. Rotilio and M. R. Ciriolo, *J. Biol. Chem.*, 2007, **282**, 12010-12021.

55. V. Farfariello, S. Liberati, M. B. Morelli, D. Tomassoni, M. Santoni, M. Nabissi, A. Giannantoni, G. Santoni and C. Amantini, *Chem.-Biol. Interact.*, 2014, **224**, 128-135.

56. M. Garrido-Armas, J. C. Corona, M. L. Escobar, L. Torres, F. Ordóñez-Romero, A. Hernández-Hernández and F. Arenas-Huertero, *Toxicol. In Vitro*, 2018, **51**, 63-73.

57. C. Marzano, V. Gandin, M. Pellei, D. Colavito, G. Papini, G. G. Lobbia, E. Del Giudice, M. Porchia, F. Tisato and C. Santini, *J. Med. Chem.*, 2008, **51**, 798-808.

View Article Online
DOI: 10.1039/C8NJ01763H

Novel antitumor copper(II) complexes rationally designed to act through synergistic mechanisms of action, due to the presence of an NMDA receptor ligand and copper in the same chemical entity

Table of contents:

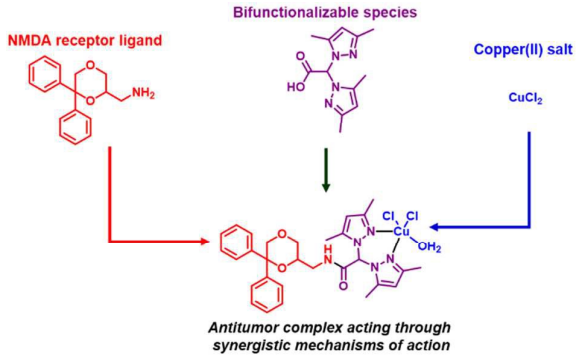

An NMDA receptor ligand was linked to bifunctionalizable species to form copper(II) complexes, showing antitumor activity through synergistic action mechanisms.